Effects of damage rate on Cu precipitation in Fe–Cu model alloys under neutron irradiation

AUTHOR(S):

Xu, Q.; Yoshiie, T.

CITATION:

Xu, Q. ...[et al]. Effects of damage rate on Cu precipitation in Fe–Cu model alloys under neutron irradiation. Philosophical Magazine 2011, 91(28): 3716-3726

ISSUE DATE:

2011-07-08

URL:

http://hdl.handle.net/2433/158033

Effects of Damage Rate on Cu Precipitation in Fe-Cu Model Alloys under Neutron Irradiation

Q. Xu and T. Yoshiie

Research Reactor Institute, Kyoto University, Osaka 590-0494, Japan

Abstract

The formation of Cu precipitates and point defect clusters was investigated in two Fe-Cu binary model alloys, Fe-0.3Cu and Fe-0.6Cu, irradiated at 573 K at three different damage rates, namely 3.8×10^{-10}, 1.5×10^{-8} and 5×10^{-8} dpa (displacements per atom)/s, up to about 1.6×10^{-2} dpa. Results of positron annihilation experiments indicated that Cu precipitates were formed in these irradiations with different damage rates. The growth of Cu precipitates does not increase monotonously with increasing irradiation dose, but it rather depends on the nucleation and growth of microvoids. It is also clear that the nucleation and growth of microvoids are influenced by the irradiation dose rate.

PACS number(s): 61.82.Bg, 78.70.Bj, 81.30.Mh

1. Introduction

Cu precipitates form in Fe-Cu alloys during thermal aging at high temperatures, as well as upon irradiation with high energy particles [1, 2], since Cu atoms are almost insoluble in α-Fe. Cu precipitates obstruct dislocation motion during deformation, which increases the hardness and decreases the ductility of the alloy, thus inducing embrittlement in Fe-based alloys containing Cu impurities, such as old commercial reactor pressure vessel (RPV) steels. Besides Cu precipitates, defect clusters, such as interstitial clusters and vacancy clusters, are also formed during irradiation, which are further contributing factors to increasing hardness and decreasing ductility of RPV steels.

In order to develop new RPV steels and to estimate the lifetimes of RPV steels used in present nuclear power plants, accelerated irradiation with neutrons, ions and electrons is typically employed, wherein the damage rate is higher than the actual damage rates experienced in nuclear power plants. Thus, the damage rate is thought to be another important factor influencing the formation of Cu precipitates in Fe-Cu alloys. The effects of damage rate on the nucleation and growth of voids and interstitial-type dislocation loops has been studied experimentally and theoretically [3-10]. For example, peak temperature of swelling increases with increasing damage rate for void formation. For the formation of interstitial-type dislocation loops, experiments and simulations have shown that the number density of loops is proportional to the square root of the damage rate [11]. Though the effects of damage rate on formation of Cu precipitates in Fe-Cu alloys have been investigated by the experiments and calculations [12, 13], and the difference in formation of Cu precipitates is clear in irradiation with difference damage rates, the details on process of Cu precipitates, which is dominated by the damage rate, is still not clear.

Positron annihilation spectroscopy is a powerful tool for detecting vacancy-type defects in condensed matter [14]. Doppler broadening of positron annihilation radiation is a nondestructive technique for testing defect clusters. In the dominant decay mode of a thermal positron and electron, two gamma rays are emitted. In the laboratory frame, the energies of the two photons emitted by the annihilation of a positron and electron are different. This difference in photon energy is proportional to the longitudinal component of the electron-positron momentum in the direction of gamma emission. Through the measurement of photon energies, information about the momentum distribution of core electrons can be obtained. Thus, Doppler broadening measurements can provide useful information about the distribution of elements around the annihilation site. Recently, Doppler broadening measurements were improved by using a two-Ge-detector coincidence system, which decreases the background of high momentum contributions by about two or three orders of magnitude compared with traditional measurements using a single Ge-detector [15].

The main purpose of the present study was to investigate the effects of damage rate on microstructural evolution in dilute Fe-Cu alloys, which are model alloys of RPV steels, using positron annihilation spectroscopy.

2. Experimental procedure

Two Fe-Cu alloys, Fe-0.3Cu and Fe-0.6Cu, were tested in this study. The composition of Cu is in weight percent. The model alloys were prepared from pure Fe (99.99% purity) and copper (99.9%) using a high-frequency induction furnace under vacuum. After melting, solution treatment was carried out at 1423 K for 24 h, followed by quenching in water. All specimens were rolled to a thickness of 0.1 mm, punched into 3-mm discs, annealed at

1223 K for 0.5 h in vacuum, and quenched in water. Neutron irradiation was carried out at the Kyoto University Reactor (KUR) at 573 K using three different facilities named Hydraulic Conveyer (Hyd), Material Controlled Irradiation Facility (SSS) and Slant Exposure Tube (Sl) under well-controlled temperature conditions using an electric heater. SSS is a dedicated tube for material testing, but Hyd and Sl facilities are opened for all users. The damage rates in Hyd, SSS and Sl were 5×10^{-8}, 1.5×10^{-8} and 3.8×10^{-10} dpa/s, respectively. The damage rate in the Hyd was about 130 times higher than that of Sl. The operation of irradiation experiment was easier in SSS than in Hyd and Sl, so the irradiations were carried out delicately in SSS to investigate the microstructural evolution. The irradiation doses in Hyd were 8.9×10^{-4}, 2.7×10^{-3} and 4.3×10^{-3} dpa, those in SSS were from 4×10^{-6} to 1.6×10^{-2} dpa [16], and those in Sl were 5.5×10^{-4} and 2×10^{-3} dpa. Positron lifetime and coincidence Doppler broadening (CDB) were measured at room temperature before and after irradiation. The positron lifetime spectrometer had a time resolution of 190 ps (full width at half maximum) and each spectrum was accumulated over a total of 1×10^{6} counts. To discriminate between bulk and defect components, after subtracting the source and background components, the lifetime spectrum $L(t)$ was decomposed into two components using the programs Resolution and Positronfit [17]:

$$L(t) = (I_1/\tau_1)\exp(-t/\tau_1) + (I_2/\tau_2)\exp(-t/\tau_2) \ , \qquad (1)$$

where τ_i are the lifetimes and I_i are the intensities. The long lifetime τ_2 originates from vacancies and, if any, vacancy clusters, while the short lifetime τ_1 results from the positron lifetime of free electrons and other defects, such as dislocations.

The average positron lifetime τ_m is defined as

$$\tau_m = I_1\tau_1 + I_2\tau_2 \,. \qquad (2)$$

Doppler-broadening spectra were accumulated over a total of 2.0×10^7 counts. The energy resolution was 1.4 keV at 511 keV.

3. Results

3.1 Lifetime measurements

Fig. 1 shows the lifetimes and intensities of the long lifetime τ_2 in Fe-0.3Cu irradiated at 573 K in SSS (a), as well as in Hyd (shown in right-hand figures of (b)) and Sl (shown in left-hand figures of (b)). To ascertain the size of the microvoids from the lifetimes, the calculated positron lifetimes of V_1 (single vacancy), V_3 (tri-vacancies), V_{10} (ten vacancies) and V_{15} (fifteen vacancies) in Fe determined by Puska *et al.* [18] using the superposition method are listed on the right-hand side of the figures in 1(a).

In Fig. 1(a), the lifetime spectra could not be decomposed into two components after irradiation to 4×10^{-6} dpa (point 1), and the mean lifetime was 105.5 ps, which was close to 106.4 ps, the lifetime of the unirradiated Fe-0.3Cu [19]. When the irradiation dose was increased to 1.3×10^{-5} dpa (point 2), the lifetime spectrum could be decomposed into two components. The long lifetime τ_2 was 143.3 ps with an intensity of 35.4%, which is lower than 190 ps, the lifetime of a single vacancy calculated by Puska et al. using the superposition method [18]. The long lifetime increased to 194.5 ps at a dose of 4×10^{-5} dpa (point 3), which is close to the lifetime of a single vacancy. This means that single vacancies were present. Microvoids were formed when the irradiation dose was increased to 1.2×10^{-4} dpa (point 4). Subsequently, the long lifetime increased drastically from 220 to

399 ps, which corresponds to microvoids containing 15 vacancies according to the calculation by Puska et al. [18], with doses from 4×10^{-4} to 3×10^{-3} dpa (points 5 to 7). When the irradiation dose was increased from 3×10^{-3} to 6×10^{-3} dpa (points 7, 8), there was little change in the long lifetime τ_2 (394.9 ps), and the intensity I_2 of the microvoids decreased slightly during irradiation. The long lifetime decreased from 394.9 to 184.2 ps, and the intensity I_2 increased from 9.3% to 31.3% when the irradiation dose was increased from 6×10^{-3} to 1.6×10^{-2} dpa (points 8, 9). In addition, the short lifetime τ_1 was higher than the lifetime of the unirradiated sample after irradiation to 1.2×10^{-3} dpa (point 6), where vacancy clusters were formed. The increase in the short lifetime was caused by irradiation-induced interstitial type dislocation loops. On the other hand, after irradiation to 5.5×10^{-4} dpa in Sl, as shown in Fig. 1 (b), τ_2 was 322.9 ps with intensities of 11.6%, which corresponded to V_{10}. The short lifetime τ_1 was 110.0 ps, which is higher than the lifetime of the unirradiated sample, due to irradiation-induced interstitial-type dislocation loops. As the irradiation dose was increased to 2×10^{-3} dpa, τ_1 and τ_2 increased slightly, but intensity of the long lifetime τ_2 increased prominently. The long lifetime τ_2 was 154.7 ps, which is lower than the lifetime of a single vacancy (190 ps), and stemmed from dislocations and monovacancies trapped by the dislocations, after irradiation to 8.9×10^{-4} dpa in Hyd. As the irradiation dose was increased to 2.7×10^{-3} dpa, τ_2 increased rapidly to 341.1 ps, which corresponds to V_{10}, and τ_1 increased as well, up to 118.1 ps, the lifetime of dislocations [20]. Subsequently, τ_2 decreased from 341.1 to 274.8 ps when the irradiation dose was increased from 2.7×10^{-3} to 4.3×10^{-3} dpa, whereas there was little change in τ_1.

Fig. 2 shows the lifetimes and intensities of the long lifetime τ_2 in Fe-0.6Cu irradiated at 573 K in the SSS (a), and in Hyd (right-hand figures in (b)) and Sl (left-hand figures in (b)). As shown in Fig. 2 (a), changes in the long lifetime and density as a function of

irradiation dose in Fe-0.3Cu and Fe-0.6Cu are almost the same in SSS, though the long lifetime in Fe-0.6Cu was lower than 190 ps, the lifetime of a single vacancy, during the irradiation from 4×10^{-5} to 1.2×10^{-4} dpa (points 3',4'). The long lifetime was higher than the lifetime of a single vacancy when the irradiation dose increased to 4×10^{-4} dpa (point 5'). As with the changes in the lifetime in Fe-0.3Cu irradiated in Hyd and Sl, with increasing irradiation dose, τ_2 in Fe-0.6Cu irradiated in Sl showed minimal change, as shown in Fig. 2, whereas that in Fe-0.6Cu irradiated in Hyd increased with increasing irradiation dose from 8.9×10^{-4} to 2.7×10^{-3} dpa. τ_2 changed little when the irradiation dose was increased from 2.7×10^{-3} to 4.3×10^{-3} dpa. τ_2 was lower in Fe-0.6Cu irradiated in Hyd than in Fe-0.3Cu.

As a reference, the lifetimes and intensities of the long lifetime τ_2 in pure Fe irradiated at 573 K in Hyd and Sl are shown in Fig. 3. The long lifetime increased and its intensity tended to decrease with increasing irradiation dose in both cases. The long lifetime τ_2 (305 ps) in Sl after irradiation to 2×10^{-3} dpa was higher than that (294 ps) in Hyd after irradiation to 4.3×10^{-3} dpa, though the irradiation dose in the latter case was higher. In addition, the intensity of long lifetime decreased with decreasing damage rate.

3.2 Coincidence Doppler broadening measurement

In the present study, we introduced two parameters, namely S and W, which are defined as the ratio of the low-momentum ($|P_L| < 4\times10^{-3}\ m_0c$) and high-momentum ($20\times10^{-3}\ m_0c < |P_L| < 30\times10^{-3}\ m_0c$) regions in the Doppler broadening spectrum to the total region, respectively. S represents the smaller Doppler shift resulting from annihilation of valence electrons. In the same material, when compared with a well-annealed sample, the increase in S comes from the positron annihilation at vacancy-type defects. So, the increase in the size or density of vacancies causes the S to increase. W comes from annihilation at core

electrons, which is used to estimate the number of Cu atoms around positrons when they are annihilated. The increase in size or density of Cu precipitates also increases W. The changes in S and W are not independent. Only the change in size and density of microvoids or precipitates can change both S and W, since S and W are defined as the ratio of certain regions in the Doppler broadening spectrum to the total region.

S-W plots in Fe-0.3Cu and Fe-0.6Cu irradiated in SSS, Hyd and Sl are shown in Figs. 4 and 5, respectively, wherein our other data for unirradiated Cu, Fe, Fe-0.3Cu and Fe-0.6Cu are shown. In addition, data for irradiated Fe are also included for comparison, which were obtained by irradiation at the Japan Material Testing Reactor (JMTR), where the irradiation temperature was 563 K, and the doses were 3.9×10^{22}, 1.8×10^{23}, 3×10^{23} and 8.2×10^{23} n/m^2, corresponding to 9.6×10^{-3}, 4.4×10^{-2}, 7.4×10^{-2} and 0.2 dpa, respectively. The lifetime results of irradiated Fe show that microvoids grew with increasing irradiation dose. The (S, W) points of irradiated Fe (a, b, c and d) were aligned on the same line segment, which meant that S increased and W decreased with increasing microvoid size since the fraction of positrons annihilated at the microvoids increased. It is also clear that the changes of S and W are not independent. In Fe, where precipitates do not exist, W decreases and does not remain the same, with increasing microvoid size. In the Fe-0.3Cu alloy irradiated in SSS, a change in S and W was initiated when the irradiation dose was increased to 1.3×10^{-5} and 4×10^{-5} dpa, respectively, corresponding to points 2 and 3 in Fig. 4. With increasing irradiation dose from 4×10^{-5} (point 3) to 4×10^{-4} dpa (point 5), both S and W increased; the increase in W was not significant from 4×10^{-4} (point 5) to 1.2×10^{-3} dpa (point 6). Beyond this dose, W continued to increase but S decreased (points 6 to 9). Comparing with the lifetime results shown in Fig. 1, the increase in S corresponded to the formation of vacancies (point 3) or growth of microvoids (points 4 to 6), while the subsequent decrease

in S corresponded to a decrease in the microvoid size or density (points 6 to 9). In Hyd irradiation, with increasing irradiation dose from 8.9×10^{-4} to 2.7×10^{-3} dpa (points 1H and 2H), S and W increased. However, when the irradiation dose increased from 2.7×10^{-3} to 4.3×10^{-3} dpa (points 2H and 3H), S decreased but W increased. Meanwhile, S increased and W decreased in Sl irradiation, though the irradiation dose in Sl was lower than that in Hyd irradiation. The (S, W) points of Fe-0.3Cu irradiated by Sl irradiation (1S, 2S) were aligned on a line segment, the slope of which was the same as that of the irradiated Fe.

Cu precipitates were formed in Fe-0.6Cu even after SSS irradiation to just 4×10^{-6} dpa (point 1'), as shown in Fig. 5, since the W value was higher than that of the unirradiated sample. Initially, W and S increased with increasing irradiation dose from 4×10^{-6} to 4×10^{-5} dpa (points 1' to 3'). From 4×10^{-5} to 3×10^{-3} dpa (points 3' to 7'), W changed little, whereas S increased. Finally, from 3×10^{-3} to 1.6×10^{-2} dpa (points 7' to 9'), W increased but S decreased. Comparing with the lifetime results shown in Fig. 2, the long lifetime increased from 118.1 ps to 151.6 ps during irradiation from 1.3×10^{-5} to 1.2×10^{-4} dpa (point 2' to 4'). The increase in S is a result of the production of vacancies, though the vacancies could not be detected by positron annihilation in the present study owing to their low density. The nucleation and growth of microvoids induced the increase in S during irradiation from 4×10^{-4} to 3×10^{-3} dpa (points 5' to 7'). The shrinkage of microvoids induced the decrease in S during irradiation from 3×10^{-3} to 1.6×10^{-2} dpa (points 7' to 9'). On the other hand, changes in S and W with increasing irradiation dose in Hyd and Sl were similar to those in Fe-0.3Cu. Comparing Figs. 4 and 5, W of Fe-0.6Cu was larger than that of Fe-0.3Cu at the same doses indicating that the fraction of annihilation at Cu precipitates was higher in the Cu-rich alloy.

4. Discussion

The mechanism of microstructural evolution in Fe-Cu alloys during neutron irradiation is important for investigating the effect of damage rate on the degradation of mechanical properties of RPV steels. In SSS irradiation, the lifetime and CDB results indicate that the formation of microvoids and Cu precipitates are different in Fe-0.3Cu and Fe-0.6Cu only in the initial irradiation stages. In Fe-0.3Cu, Cu precipitates and microvoids were formed at doses of 4×10^{-5} dpa (point 3 in Fig. 4) and 1.2×10^{-4} dpa (point 4 in Fig. 1), respectively. In Fe-0.6Cu, Cu precipitates were formed even at a dose of 4×10^{-6} dpa (point 1' in Fig. 5), and microvoids were formed at a dose of 4×10^{-4} dpa (point 5' in Fig. 2), though there was little change in W after irradiation to 4×10^{-5} dpa (point 3' in Fig. 5). These results indicate that microvoids are nucleated after the completion of Cu precipitate nucleation in Fe-0.6Cu, whereas in Fe-0.3Cu, microvoids are nucleated during Cu precipitate nucleation. Xu et al. pointed out that vacancies produced by irradiation are trapped by Cu atoms to form Cu-vacancy complexes during the initial irradiation. Subsequently, Cu clusters are formed. The concentration of Cu clusters increases with irradiation dose in the initial irradiation. As the concentration of Cu clusters, which are trapping sites for vacancies, increased, Cu cluster-vacancies complexes, i.e., vacancies nucleating at Cu precipitates, were formed [21]. The nucleation of Cu precipitates in our study agrees with this statement. Cu precipitates nucleate by vacancy migration before the formation of microvoids. The microvoids are formed by migration of free vacancies, and their density increases with increasing density of free vacancies. In Fe-0.6Cu, the Cu content is higher and the density of free vacancies in the matrix is lower because most of the vacancies in this case are trapped by Cu precipitates or Cu atoms. Microvoids are formed when the total density of vacancy trapping sites, that is, Cu precipitates and Cu atoms, decreases. Microvoids are formed in Fe-0.3Cu during

nucleation of Cu precipitates due to the high density of free vacancies. After irradiation to 4×10^{-4} dpa, the difference in microstructure evolution in the two alloys was not significant. The microvoids grew in both Fe-Cu alloys for irradiation from 4×10^{-4} to 3×10^{-3} dpa (points 5 to 7 or 5' to 7' in Figs. 4 and 5, respectively), whereas W did not change significantly. In other words, the rapid growth of microvoids occurred after the nucleation of Cu precipitates. When the irradiation dose was increased to 6×10^{-3} dpa (point 8 or 8' in Figs. 4 and 5, respectively), the microvoids shrank and aggregation of Cu atoms was promoted at the microvoids. According to the experimental results of the SSS irradiation, the formation of microvoids and Cu precipitates in Fe-Cu alloys can be summarized as follows. There are three stages in the formation of Cu precipitates up to a dose of 1.6×10^{-2} dpa. First, Cu precipitates are formed by vacancy migration (stage I). Second, vacancies nucleate at Cu precipitates and microvoids grow (stage II). As shown in Figs. 4, 1 and 5, 2, the formation of Cu precipitates and microvoids was initiated at doses of 4×10^{-5} (3) and 1.2×10^{-4} dpa (4) in Fe-0.3Cu, respectively. On the other hand, Cu precipitates were formed after irradiation to 4×10^{-6} dpa (1'), and the formation of microvoids was initiated at a dose of 4×10^{-4} dpa (5') in Fe-0.6Cu. Only S increases during the growth of microvoids. Third, the aggregation of Cu atoms is promoted at these microvoids (stage III; dose > 1.2×10^{-3} dpa (6) in Fe-0.3Cu, dose > 3×10^{-3} dpa (7') in Fe-0.6Cu, respectively), where W increases and S decreases due to the aggregation of Cu atoms at the microvoids. Cu atoms aggregated on the microvoid surfaces have also been reported [22].

Next, we discuss the effect of damage rate on the formation of microvoids and Cu precipitates in Fe-Cu alloys. Lifetime results show that in the initial irradiation to 4×10^{-4} - 8.9×10^{-4} dpa, V_{10} and V_3 microvoids were formed in the Sl and SSS irradiations, respectively, but no microvoids were formed by the Hyd irradiation in both Fe-Cu alloys

even though the irradiation dose was high in the latter case. It is clear that the onset of microvoid growth stage is early with decreasing damage rate. Generally, the concentrations of interstitials and vacancies are higher for higher damage rates, which lead to higher ratios of recombination of interstitials and vacancies in irradiation at higher damage rates. The high density of interstitials and vacancies prevents these defects from migrating over long distances, and hence, prevents defect clusters from growing large. The formation of microvoids in Fe as shown in Fig. 3 also agrees with this common knowledge, where the size of microvoids was smaller in the Hyd irradiation with high damage rate than those in the Sl irradiation with low damage rate. In both the Fe-Cu alloys in this study, τ_2 increased with increasing irradiation dose in the SSS and Hyd irradiations from 8.9×10^{-4} to 3×10^{-3} dpa. In the case of the Sl irradiation, however, τ_2 remained almost constant in both Fe-Cu alloys, but its density increased with increasing irradiation dose. This suggests that microvoid growth is complete even after irradiation to 5.5×10^{-4} dpa in Sl irradiation.

Comparing the dose dependence of the formation of microvoids and Cu precipitates in Fe-Cu alloys irradiated in Hyd, SSS and Sl, it is clear that the formation of Cu precipitates in Fe-0.3Cu and Fe-0.6Cu irradiated in Hyd to 8.9×10^{-4} dpa is stage I and to 4.3×10^{-3} dpa is stage III, since W is higher and S is lower for the 4.3×10^{-3} dpa irradiation than that of the 2.7×10^{-3} dpa irradiation. In stage I, microvoids were not formed and the increase in W was due to the precipitates nucleated by vacancy migration. In stage III, the increase in W and the decrease in S stemmed from Cu aggregation on microvoids and the shrinkage of microvoids, respectively. On the other hand, the formation of Cu precipitates in Fe-0.3Cu and Fe-0.6Cu irradiated in Sl to 5.5×10^{-4} and 2×10^{-3} dpa is stage II. The (S, W) points of both alloys (1S, 2S) and (1S', 2S') were aligned on a line segment, the slope of which was the same as that of irradiated Fe. The increase in S was due to the increase in intensity of

microvoids. In addition, the dose of point 6 (1.2×10^{-3} dpa), which is stage III, in SSS irradiation was lower than that of point 2S (2×10^{-3} dpa), which is stage II, in Sl irradiation, as shown in Fig. 4.

The effects of damage rate on the formation of microvoids are simple in pure Fe, where density of microvoids increases but size of microvoids decreases with increasing damage rate. However, the processes of formation of microvoids and Cu precipitates are complicated in Fe-Cu alloys. The nucleation and growth of microvoids depend on not only damage rate but also the nucleation and growth of Cu precipitates. The growth of Cu precipitates also depends on the growth of microvoids. In Fe-Cu alloys, as previously described, Cu precipitates nucleate by vacancy migration during the initial irradiation (stage I). Subsequently, microvoids nucleate at Cu precipitates and grow with irradiation dose (stage II). Finally, Cu precipitates grow at microvoids (stage III). According to the processes of nucleation and growth of Cu precipitates, we obtain three conclusions in the present work. First, the nucleation of Cu precipitates is accelerated with decreasing damage rate in the initial irradiation (V_{10} microvoids were formed in the Sl irradiation to 5.5×10^{-4} dpa (stage II), but no microvoids were formed in the Hyd irradiation to 8.9×10^{-4} dpa (stageI)). Second, the onset of microvoid growth stage is early with decreasing damage rate in the initial irradiation. Third, the growth of Cu precipitates is delayed with decreasing damage rate. In other words, the process of Cu precipitate formation is slower with decreasing damage rate (Cu precipitates grew in the SSS irradiation at the dose higher than 1.2×10^{-3} dpa (Fig. 4, point 6; stage III), but they did not grew in the Sl irradiation to 2×10^{-3} dpa (Fig. 4, point 2S; stage II)). Vacancies migrate in the matrix for a longer time with decreasing damage rate. This influences the precipitation of other impurities in RPV steels, such as P, S and Si, which enhances embrittlement of RPV steels if these impurities

segregate on grain boundaries. An atom probe field ion microscopy study has shown that copper atoms are mainly distributed in the core of a cluster, while Si and other impurities exhibit spatial distribution around the center of the cluster [23]. Thus, with decreasing damage rate, segregation of impurities at grain boundaries (enhancing embrittlement of RPV steels) will increase since vacancies migrating over long distances enhance diffusion of solute atoms. The effects of damage rate on evolution of dislocation loops and voids in stainless steels can be estimated using rate theory [24]. However, thus far, there has not been a useful method to predict the formation of Cu precipitates and segregation in Fe-Cu alloys. Therefore, one must be careful when estimating the lifetime of PRV steels using the accelerated irradiation data.

5. Conclusion

Two Fe-Cu alloys, Fe-0.3Cu and Fe-0.6Cu, were irradiated with fission neutrons at 573 K at three different damage rates (3.8×10^{-10}, 1.5×10^{-8} and 5×10^{-8} dpa/s) to investigate microstructural evolution. The present results clearly show that the nucleation and growth of Cu precipitates are influenced by the damage rate, but the process is very complicated as they are also related to the nucleation and growth of microvoids. The nucleation of Cu precipitates increases with decreasing damage rate, but the growth of Cu precipitates increases with increasing damage rate. In addition, the results indicate that embrittlement of RPV steels increases with decreasing damage rate.

Acknowledgments

This work was partly supported by a Grant-in-Aid for Scientific Research of the Ministry of Education, Science and Culture, under Contract No. 20560773.

References

[1] J.T. Buswell, C.A. English, M.G. Hetherington, W.J. Phythian, G.D.W. Smith and G.M. Worrall, Effects of Radiation on Materials: 14th International Symposium, ASTM STP, edited by N.H. Packan, R.E. Stoller and A.S. Kumar (American Society for Testing and Materials, Philadelphia, 1990) Vol. II, p. 127.

[2] P.J. Othen, M.L. Jenkins, G.D.W. Smith and W.J. Phythian, Phil. Mag. Lett,. 64, 383 (1991).

[3] L. Glowinski, C. Fiche and M. Lott, J. Nucl. Mater., 47 (1973) 232.

[4] J.E. Westmoreland, J.A. Sprague, F.A. Smidt and P.R. Malmberg, Rad. Effects, 26 (1975) 1.

[5] N.H. Packan, K. Farrell and J.O. Stiegler, J. Nucl. Mater., 78 (1978) 143.

[6] A.D. Brailsford and R. Bullough, J. Nucl. Mater., 44 (1972) 121.

[7] L.K. Mansur, J. Nucl. Mater., 78 (1978) 156.

[8] Q. Xu, H.L. Heinisch and T. Yoshiie, J.Comput-Aided Mater., 6 (1999) 215.

[9] S.Yanagita, T.Yoshiie and H.Ino, J. Japan. Inst. Metals 64 (2000) 115.

[10] S.Yanagita, Q.Xu,T. Yoshiie, H.Ino, Mater. Trans. 43 (2002) 1663.

[11] T. Muroga, Y. Miyamoto, H. Watanabe and N. Yoshida, J. Nucl. Mater. 155-157 (1988) 810.

[12] Y. Nagai, T. Toyama, Y. Nishiyama, M. Suzuki, Z. Tang and M. Hasegawa, Appl. Phys. Lett. 87 (2005) 261920.

[13] P.R. Monasterio, B.D. Wirth and G.R. Odette, J. Nucl. Mater. 361 (2007) 127.

[14] A. Dupasquier and A.P. Mills, Jr., Positron Spectroscopy of Solids (IOS Press, Amsterdam, 1995).

[15] P. Asoka-Kumar, M. Alatalo, V.J.Ghosh, A.C. Kruseman, B. Nielsen and K.G. Lynn, Phys. Rev. Lett. Vol 77, 2097 (1996).

[16] Q. Xu, K. Sato and T. Yoshiie, Phil. Mag. Lett. 88 (2008) 353.

[17] P. Kirkegaard, M. Eldrup, O.E. Morgensen, and N.J. Pedersen, Comput. Phys. Commun. 23, 307 (1981).

[18] M.J. Puska and R.M. Nieminen, J. Phys. F: Met. Phys. 13, 333 (1983).

[19] Q. Xu and Yoshiie, Mater. Sci. Forum 445 (2004) 216.

[20] Y. Kamimura, T. Tsutsumi and E. Kuramoto, Phys. Rev. B 52 (1995) 879, and errata same authors as above, Phys. Rev. B 54 (1996) 12595.

[21] Q. Xu, T. Yoshiie and K. Sato, Phys. Rev. B 73 (2006) 134115.

[22] Y. Nagai, Z. Tang, M. Hasegawa, T. Kanai and M. Saneyasu, Phys. Rev. B 63 (2001) 134110.

[23] K. Dohi, K. Nishida, A. Nomoto, N. Soneda and H. Watababe, J. Japan Inst. Metals, 74 (2010) 191.

[24] Y. Katoh, R. Stoller, Y. Kohno and A. Kohyama, J. Nucl. Mater. 210 (1994) 290.

Figure Captions

Fig. 1 Positron lifetimes and intensities of long lifetime in Fe-0.3Cu irradiated at three different damage rates.

Fig. 2 Positron lifetimes and intensities of long lifetime in Fe-0.6Cu irradiated at three different damage rates.

Fig. 2 Positron lifetimes and intensities of long lifetime in pure Fe irradiated at two different damage rates.

Fig. 4 S-W plot in Fe-0.3Cu at 573 K. Points 1 to 9 correspond to an irradiation dose of 4×10^{-6}, 1.3×10^{-5}, 4×10^{-5}, 1.2×10^{-4}, 4×10^{-4}, 1.2×10^{-3}, 3×10^{-3}, 6×10^{-3} and 1.6×10^{-2} dpa, respectively. In addition, a, b, c and d represent irradiation doses of 9.6×10^{-3}, 4.4×10^{-2}, 7.4×10^{-2} and 0.2 dpa in Fe irradiated in the JMTR at 563 K.

Fig. 5 S-W plot in Fe-0.6Cu at 573 K. Points 1’ to 9’ correspond to an irradiation dose of 4×10^{-6}, 1.3×10^{-5}, 4×10^{-5}, 1.2×10^{-4}, 4×10^{-4}, 1.2×10^{-3}, 3×10^{-3}, 6×10^{-3} and 1.6×10^{-2} dpa, respectively. In addition, a, b, c and d represent irradiation doses of 9.6×10^{-3}, 4.4×10^{-2}, 7.4×10^{-2} and 0.2 dpa in Fe irradiated in the JMTR at 563 K.

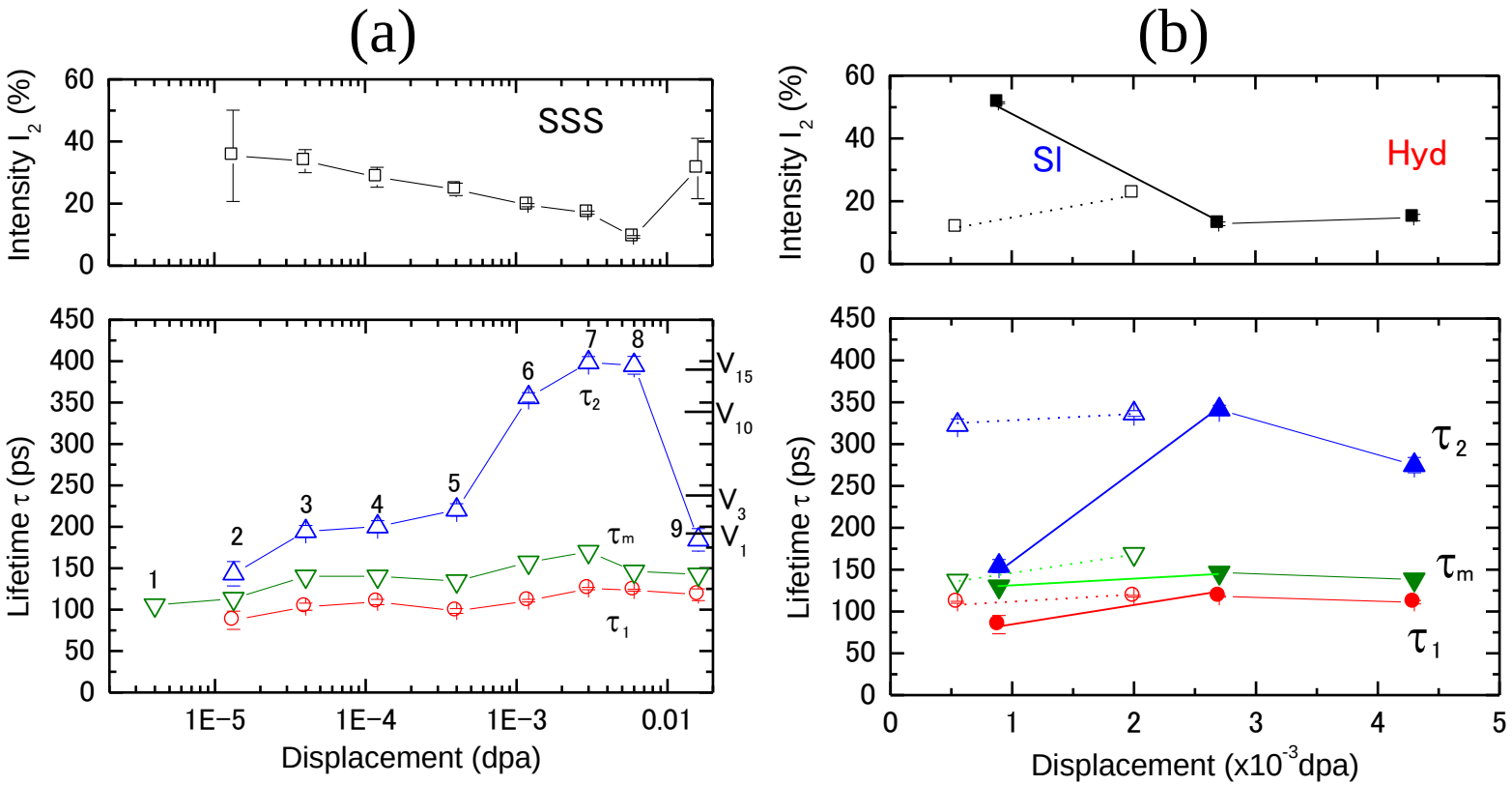

Fig. 1

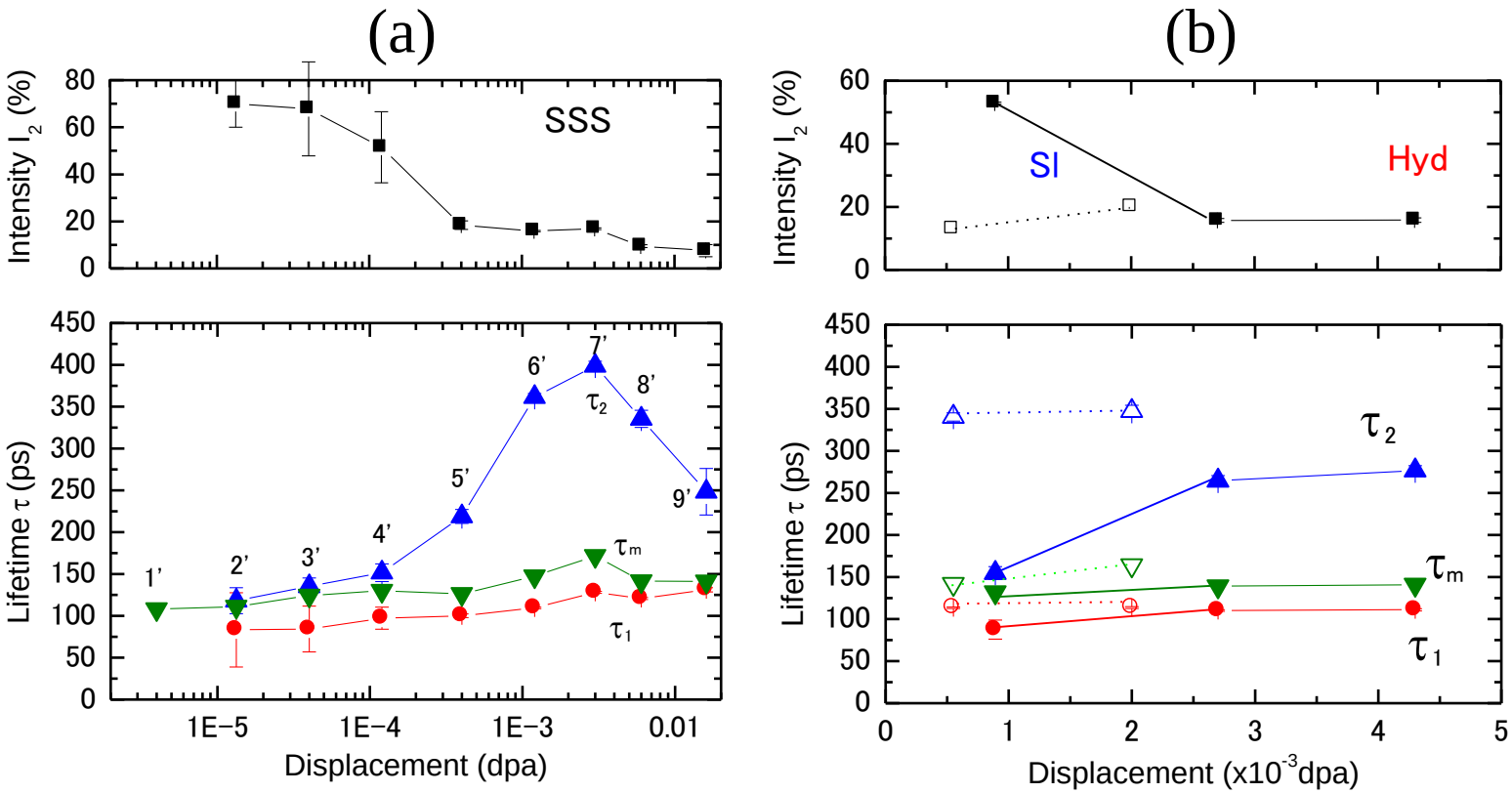

Fig. 2

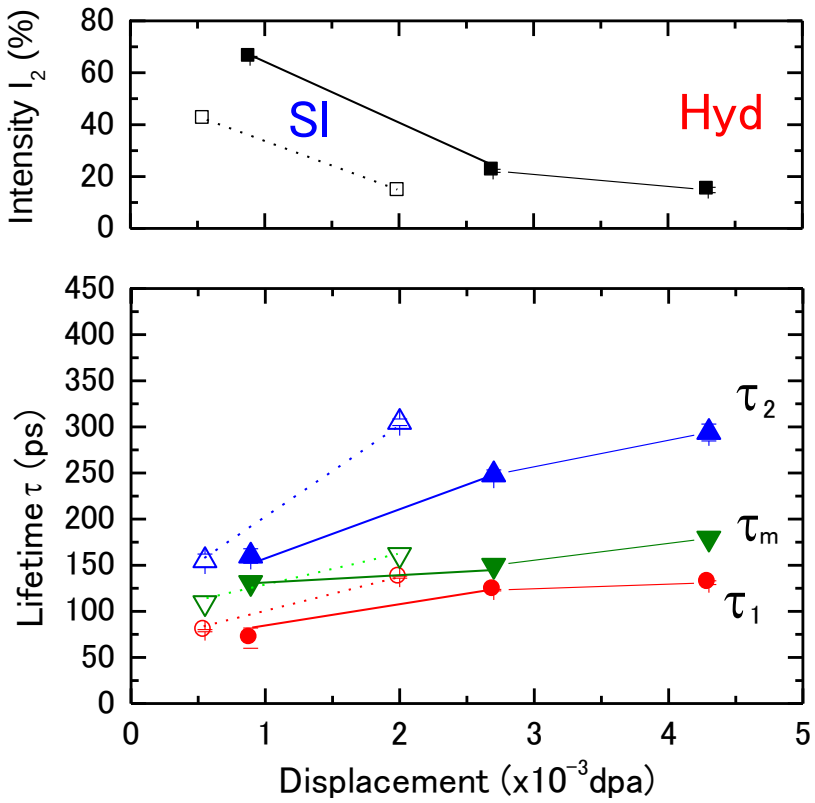

Fig. 3

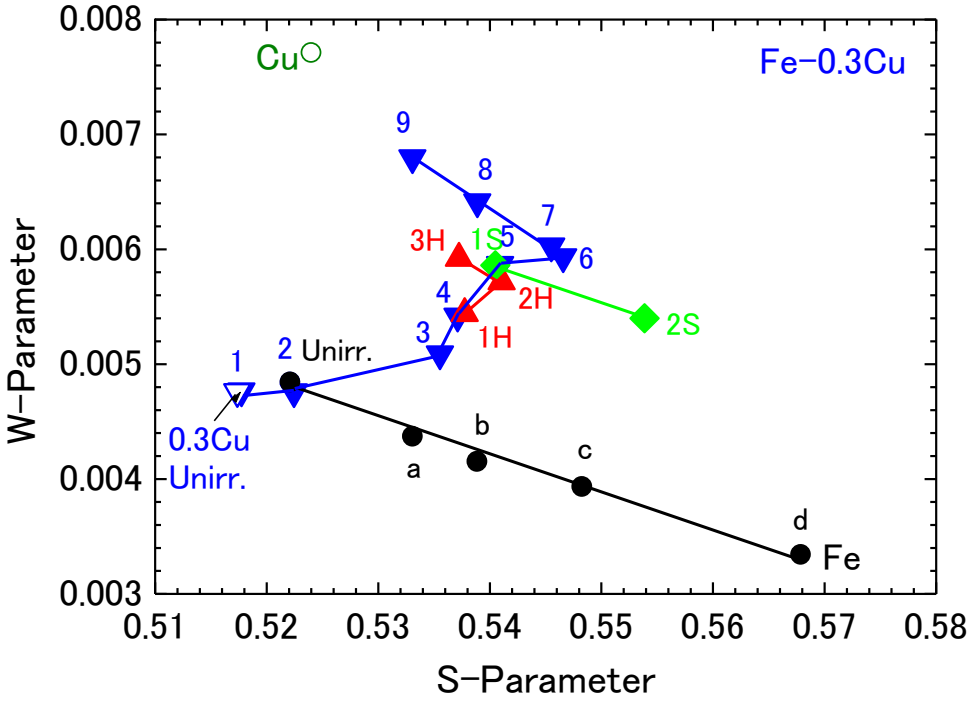

Fig. 4

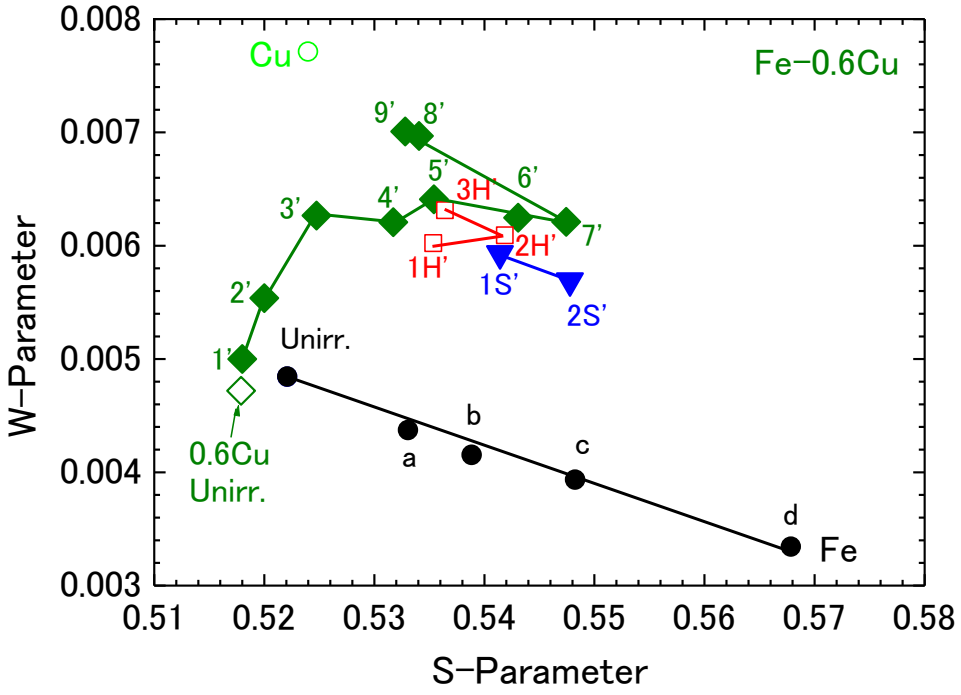

Fig. 5